

The Effect of Two-stage Heat Treatment Temperatures on Initial and FSSWed Properties of TRIP Steels

A. Mostafapour ¹, A. Ebrahimpour ^{2*}

^{1,2} Faculty of Mechanical Engineering, University of Tabriz

Abstract

In this paper, a 0.2 C–1.6 Mn–1.5 Si wt.% TRIP-aided cold-rolled steel sheet was fabricated and the optimal heat treatment conditions (Intercritical Annealing “IA” and Bainitic Isothermal Transformation “BIT”) were investigated to maximize the volume fraction and stability of the retained austenite. The effects of temperature on IA (770, 790 and 810 °C) and BIT (330, 350 and 370 °C) were studied via optical microscopy, SEM and XRD. Its tensile properties and formability were also evaluated. It is obtained that under conditions of 790 °C /330 °C and 770 °C /350 °C, the maximum and minimum amounts of the retained austenite resulted in a microstructure. Also, for the case which heat treated under 790 °C /330 °C condition obtained the best formability by showing the highest elongation (more than 40%) and the case that heat treated under 810 °C /350 °C condition had the highest tensile strength (more than 800 MPa). The cases with the maximum (12.1%) and minimum (8.1%) volume fraction of the retained austenite were chosen to investigate the effect of initial microstructure on weldability of TRIP steels. Therefore these cases were joined by friction stir spot welding process under the same welding parameters. According to the microstructural observations, four different zones determined in the welding region: stir zone, thermomechanically affected zone and high and low temperature heat affected zones. It is obtained that the steel with higher amount of the retained austenite in initial microstructure shows better mechanical properties before and after FSSW process because of higher amount of the retained austenite which causes TRIP effect.

Keywords: TRIP steel; Friction stir spot welding; Heat treatment; Retained austenite; Microstructure.

1. Introduction

There is an increasing interest concerning the application of transformation induced plasticity (TRIP) steels in automotive industry because of their good combination of high strength and formability due to the existence of the retained austenite in their microstructures, which transforms to the martensite phase during deformation ¹⁾. Therefore, there is an increasing demand to join them. Unfortunately, the fusion welding processes destroy the initial microstructure and eliminate the retained austenite in the weld area of TRIP steels, and therefore decrease the related strength and ductility ^{2, 3)}.

Friction stir welding (FSW) was invented at The Welding Institute of the UK in 1991 ⁴⁾.

This joining method is fundamentally a solid state process without large distortion, solidification cracking, porosity and other defects arising from conventional fusion welding. Furthermore, friction stir spot welding (FSSW) base on fundamentals of FSW as a new spot welding method can be used to join overlapping workpieces and proposes to replace the resistance spot welding. This method consists of only the plunge, dwell and retract stages of FSW ^{5, 6)}.

FSSW was initially limited to join aluminum alloy but with the development of new suitable tool materials, nowadays this process can be applied to weld steels. Lakshminarayanan et al. ⁷⁾ identified the optimum friction stir spot welding process parameters by controlling the properties of low carbon automotive steel joints. Recently, some investigations have shown that the FSW/FSSW can be a promising method for joining the TRIP steels ^{2, 3, 8- 10)}.

The microstructure of TRIP steel, especially the volume fraction of the retained austenite, plays a key role on mechanical properties of steel ¹¹⁾.

* Corresponding author

Email: a.ebrahimpour@tabrizu.ac.ir

Address: Faculty of Mechanical Engineering, University of Tabriz

1. Associate Professor

2. PhD Student

The most important factors for the austenite stability appear to be its carbon-content, grain size and morphology^{12, 13}.

The microstructure of TRIP steel can be obtained by a two-stage heat treatment processing. As shown in Fig. 1, at the first stage which is known as Intercritical Annealing (IA), the steel is annealed between Ac_1 and Ac_3 in order to dissolve the original microstructure. After the IA, the steel has been rapidly cooled to a temperature between martensite start temperature (M_s) and bainite start temperature (B_s), where bainite would form. This step is also known as bainitic isothermal transformation (BIT)².

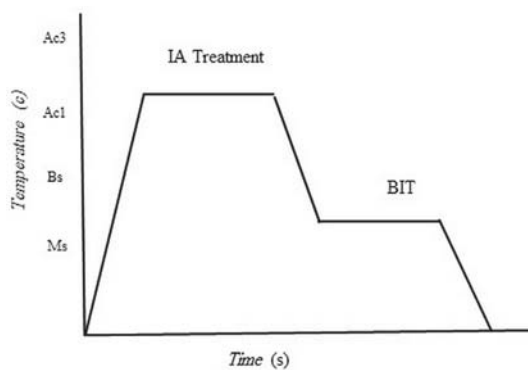


Fig. 1. Two-stage heat treatment of TRIP steels.

Also, it has been reported that the microstructure evolution during FSSW/FSW of steels is dependent on the initial microstructure^{2, 14, 15}. Ghosh et al.¹⁴ have investigated the FSW of martensitic steel and found that the microstructure of stir zone is fully martensitic due to a peak temperature in the austenitic region. Further analysis has revealed a smaller prior austenite grain size in the stir zone. In another work, Fujii et al.¹⁵ have studied the FSW of ultra-low carbon steel with an initial microstructure being fully ferritic. They have reported that the microstructure in the stir zone is fully ferritic but with a refined grain size and the grain refinement which is caused by the recovery of ferrite.

In the open literature, some studies have examined the effects of IA and BIT on the microstructure and mechanical properties of this class of materials^{11, 16-20}. However, the researchers have not considered the effect of temperature of IA (T_{IA}) on M_s and B_s , which are important parameters on the selection of temperature of BIT (T_{BIT}). T_{BIT} and its differences with M_s and B_s have important influence on bainite formation and the volume fraction of the retained austenite and its morphology.

Moreover, there are studies that have investigated the FSW/FSSWed TRIP steels mechanical and microstructural properties^{2, 3, 8-10} but, the effect of initial microstructure on weldability of TRIP steels has not been sufficiently clarified. Therefore, in

this paper the effect of IA and IBT temperatures on the microstructure and mechanical properties of TRIP steels and friction stir spot welded joints are investigated.

2. Experimental methods

The chemical composition of the TRIP steel contained 0.21 C, 1.68 Mn, 1.5 Si, 0.03 Cr, 0.01 Ni, 0.016 Al and 0.009 S (wt.%). The steel was prepared as a 5 kg ingot in an air induction furnace. The cast ingot was forged and small blocks were cut from forged stock. These blocks were soaked at 1200 °C for 1 h, and hot rolled to a thickness of 4 mm. Hot rolled plates were annealed at 900 °C for 1 h to reduce the hardness for easier cold rolling. The hot-rolled air annealed steel plates were cold rolled to achieve a final thickness of 1.2 mm.

The temperatures of Ac_1 and Ac_3 calculated using Thermo-Calc database²¹ and the amount of 705 °C and 836 °C obtained, respectively.

One of the main goals of IA treatment is the stabilization of a dual-phase microstructure with sufficient volume fraction of ferrite to result in adequate ductility of the TRIP steel as well as an austenite phase sufficiently enriched with carbon so it is stable against martensitic transformation during quenching to T_{BIT} . The selection of T_{IA} must also be sufficiently above the stability boundary for the formation of the cementite to guarantee no carbon sinks that would deplete the IA-austenite of carbon, making it more susceptible to martensitic transformation after quenching. The optimum temperature for IA has been reported as $Ac_1 + Ac_3 / 2 + 20$ °C²². In the current research, this formula predicts optimum temperature of 790 °C, but for investigation of the effect of TIA, the IA treatment has accomplished at three different temperatures of 770, 790, and 810 °C for 600 s in a 50% NaCl+50% Na_2CO_3 salt bath. The volume fraction of austenite and ferrite in this dual phase zone and the carbon content of austenite is given in Table 1 which were calculated using Fe-C diagram obtained from Thermo-Calc software. The presented amount of M_s and B_s are dependent on carbon content of austenite. These temperatures are calculated by MUCG83 software²³ and given in Table 1.

After the IA treatment, the alloy must be quenched to T_{BIT} in order to promote further C-enrichment of austenite. At this stage, the proper quenching rate and holding temperature are required to avoid the formation of cementite. At the same time, the T_{BIT} must be higher than M_s of the IA-austenite and must be lower than its B_s . In order to investigate the effect of T_{BIT} on the microstructure and mechanical properties, three amounts of 330, 350 and 370 °C selected by considering the M_s and B_s . Therefore two groups of steels were prepared by two-stage heat treatment.

Steels A, B and C corresponded to treatments with the same T_{BIT} at 350 °C and T_{IA} at 770, 790 and 810 °C, respectively and steels B, D and E, which were heat treated with different T_{BIT} at 350, 330 and 370 °C and the same T_{IA} at 790 °C. Table 2 represents the heat treatment condition in cases A to E. After BIT the samples were quenched in water to room temperature.

After heat treatment process the two TRIP steel plates, which had the maximum and minimum retained austenite in their microstructures, were prepared according to ISO14273²⁴⁾ (with dimensions of 30 mm ×100 mm ×1.2 mm) and then friction stir spot welded. The FSSW process parameters including the rotational speed, the dwell time, and the plunge depth, were set to 1200 rpm, 2 s and 2 mm, respectively. For this purpose, a special fixture was designed and fabricated, and a tool was made of tungsten carbide , as in FSSW the reaction forces on the workpiece are intense.

Optical microscopy (OM) and field emission scanning electron microscopy (FE-SEM) were used for macro and microstructure observation. Furthermore, the volume fraction of the retained austenite was measured by XRD using Cu-K α radiation. Microhardness of welding zone was measured along the lines parallel to the sheet surface, at a distance of 0.5 mm from the surface of the upper sheet. In addition, in order to record the thermal history and temperature distribution, K thermocouples of 1–2 mm-diameter were used.

Table 1. Calculated amounts of austenite and its carbon content, ferrite and thermodynamic temperatures of steels after IA.

| T _{IA} (°C) | Austenite% | Ferrite% | % C | B _s (°C) | M _s (°C) |
|----------------------|------------|----------|------|---------------------|---------------------|
| 770 | 42 | 58 | 0.51 | 422 | 255 |
| 790 | 51 | 49 | 0.41 | 479 | 310 |
| 810 | 60 | 40 | 0.34 | 505 | 340 |

Table 2. Heat treatment condition for cases A-E.

| Case | T _{IA} (°C) | IA holding time (min) | T _{BIT} (°C) | BIT holding time (min) |
|------|----------------------|-----------------------|-----------------------|------------------------|
| A | 770 | 10 | 350 | 10 |
| B | 790 | | 350 | |
| C | 810 | | 350 | |
| D | 790 | | 330 | |
| E | 790 | | 370 | |

3. Results and discussion

3.1. Two-stage heat treatment

Fig. 2 represents the FE-SEM and OM microstructures of steel B. Ferrite, bainite and retained austenite are shown in this figure. Also Fig. 3(a) shows the volume fraction of the retained austenite of the cases A, B and C, which were heat treated with different T_{IA} at 790, 770 and 810 °C and the same T_{BIT} at 350 °C. According to Table 1 carbon content of austenite (formed in stage IA), for case A (T_{IA}=770 °C) was higher than case B (T_{IA}=790 °C). It was expected that the case A shows higher thermal stability during cooling, but because of the low amount of austenite in stage IA, the volume fraction of the retained austenite in this case was less than the volume fraction of the retained austenite in case B. With increasing T_{IA} up to 810°C in case C, the volume fraction of the retained austenite decreased again, because of low carbon content of austenite at IA stage. With increasing the austenitization temperature, the austenite grains get larger and so their shear transformation to martensite would be easier. Therefore, less retained austenite will be remained in the microstructure. On the other hand, with increasing the austenitization temperature, the amount of prior austenite increases and the carbon content of it decreases. Therefore, the thermal stability of austenite decreases with increasing the austenitization temperature.

According to Fig. 3a the carbon content of the retained austenite increased at first and then with the passage of time decreased with T_{IA}. Bhadeshia²⁵⁾ increase, proposed a limit to the carbon enrichment in the retained austenite during BIT resulting from the exhaustion (due to carbon enrichment in the retained austenite) of the driving force for partitionless bainite growth. This limit is usually denoted as the T₀ line²⁶⁾.

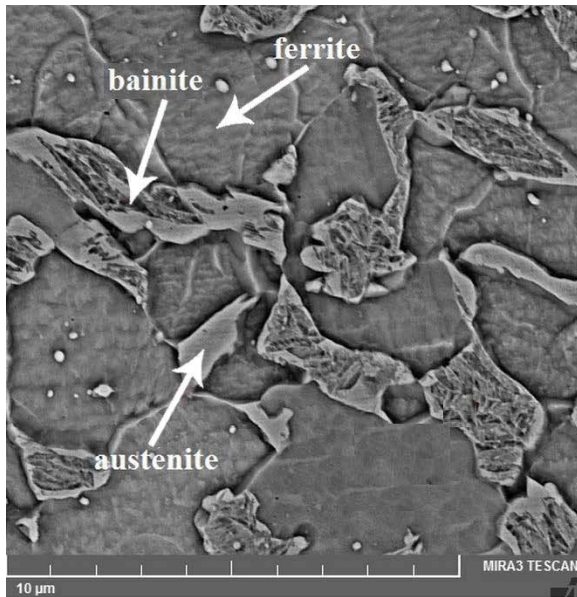
This thermodynamic limit for the transformation is further constrained when considering the energy barriers to the growth of bainite plates, estimated by Bhadeshia to be about 400 J/mol²⁵⁾. As the transformation progresses, carbon is rejected into the untransformed austenite, reducing the driving force for subsequent diffusionless growth of bainite. Once this driving force equals 400 J/mol, the bainitic transformation can no longer be sustained and the reaction stops. This thermodynamic constraint to the bainitic transformation is denoted as T'₀. Fig. 4 shows T₀ and T'₀ lines obtained from MUCG83 for T_{IA} of 790 °C. According to this figure when the difference between M_s and T_{BIT} decreases, the carbon content of the retained austenite increases.

As difference between M_s and T_{BIT} decreases with increasing T_{IA} , it is expected that the carbon content of the retained austenite increases. This is confirmed by increasing T_{IA} from case A to case B. In the case C, despite the increase in T_{IA} , the carbon content of the retained austenite decreased. This is due to a significant reduction in carbon content of the austenite formed in IA.

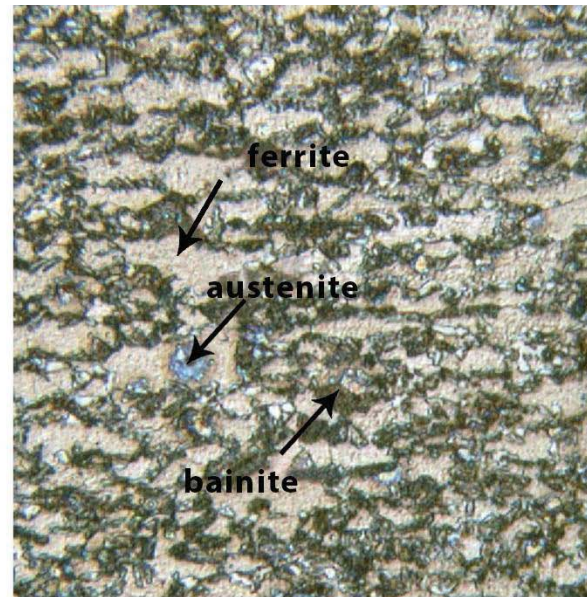
Cases B, D and E correspond to treatments with the same T_{IA} at 790 °C and T_{BIT} at 330, 350 and 370 °C, respectively. The M_s temperature for these cases is 310 °C and the difference between M_s and T_{BIT} increases

by increasing T_{BIT} . Considering the austenite volume fraction and its carbon, formed at IA, are equal for these cases and according to Fig. 4, it is expected that the volume fraction of the retained austenite and its carbon content decrease by the increase of T_{BIT} . Fig. 3b confirms this prediction.

The results of the tensile tests for cases are shown in Fig. 5. The samples A and B have the maximum and minimum tensile strength in Fig. 5a. It is due to high amount of the retained austenite. But the elongations of samples A and C are higher than sample B.



(a)



(b)

Fig. 2. Microstructure TRIP steel (case B): (a) FE-SEM micrograph and (b) OM.

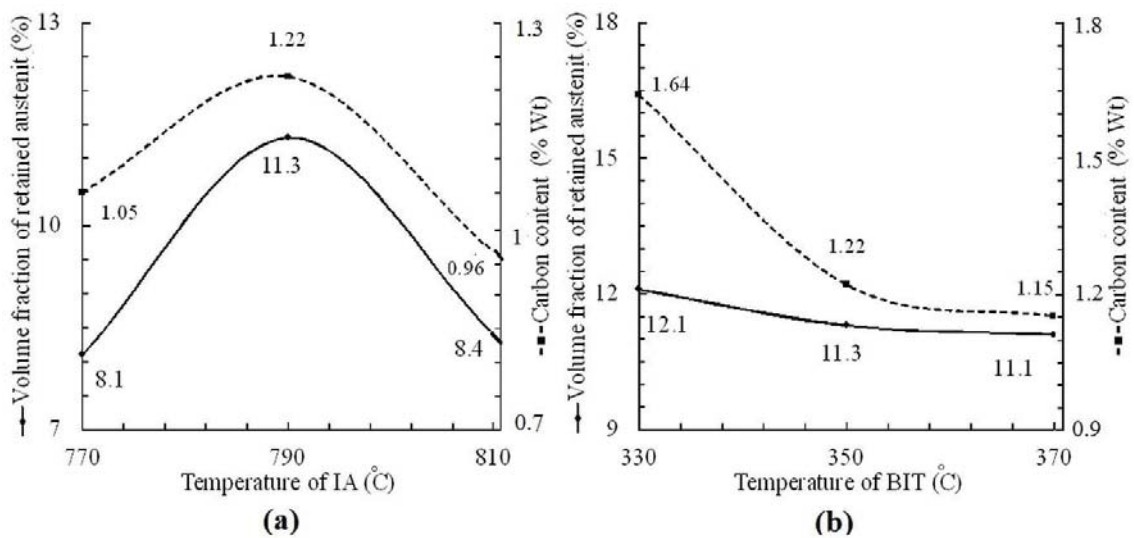


Fig. 3. Volume fractions of the retained austenite and its carbon content in: (a) cases A, B and C and (b) cases B, D and E.

The reason of this reduction in formability of case B is related to low amount of ferrite in the microstructure (see Table 1). According to Fig.5b tensile strength and elongation of cases B, D and E decrease with increasing T_{BIT} . This is due to the reduction of the volume fraction of the retained austenite and its carbon content (Fig. 3).

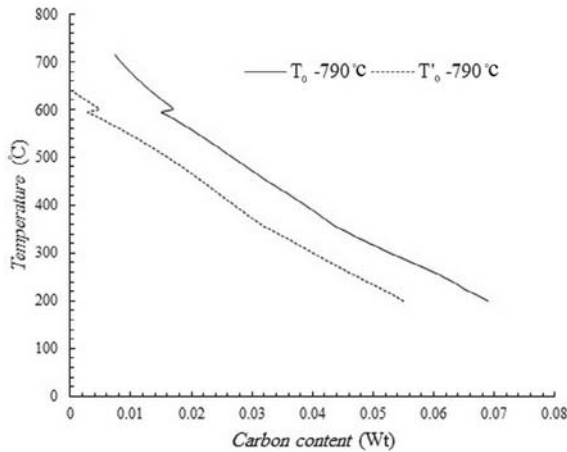


Fig. 4. T_0 and T'_0 line for $T_{IA}=790$ °C.

3.2. FSSW

Samples A and D which had the minimum (8.1%) and maximum (12.1%) amounts of the retained austenite in the microstructure and significant differences in mechanical properties, were chosen to investigate the effect of initial microstructure on friction stir spot weldability of TRIP steels.

Fig. 6 shows the section view of experimentally welded sample D which four zones can be determined on it by various colors observation. Fig. 7 shows the experimentally measured thermal history of four points from four zones that were described above. As can be seen in Fig. 7 the temperature at zones I and IV is above Ac_3 and less than Ac_1 respectively and at zones II and III is between Ac_3 and Ac_1 .

Fig. 8a shows the FE-SEM micrograph of zone (I) in case D. The formation of ferrite, bainite, martensite and martensite-austenite constituent, indicate that the temperature during the heating process was above Ac_3 , and the cooling rate was lower than the critical cooling rate for obtaining 100 % martensitic microstructure.

In the zone (I), the microstructure completely changes to austenite but there are some reports that a part of the retained austenite of the base metal stabilizes during welding in this zone^{2,14}. During welding, Austenite was exposed to a high deformation simultaneously with the high temperature, and that will probably lead to recrystallization of the austenite before it transforms into martensite or other phases.

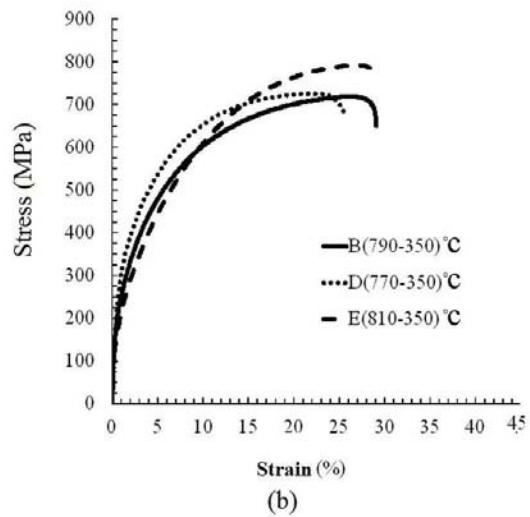
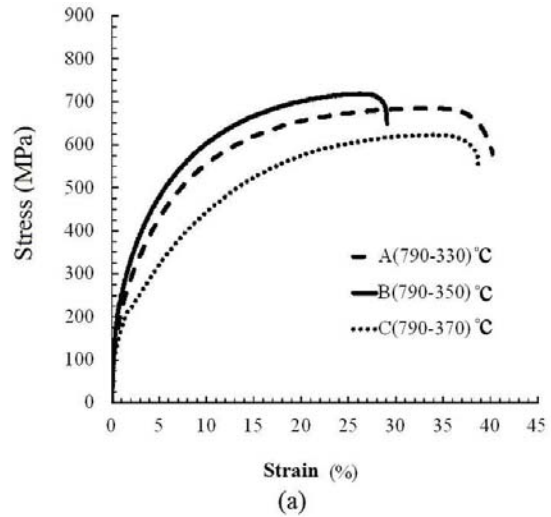


Fig. 5. Elongation-stress curves of samples (a) A, B and C and (b) B, D and E.

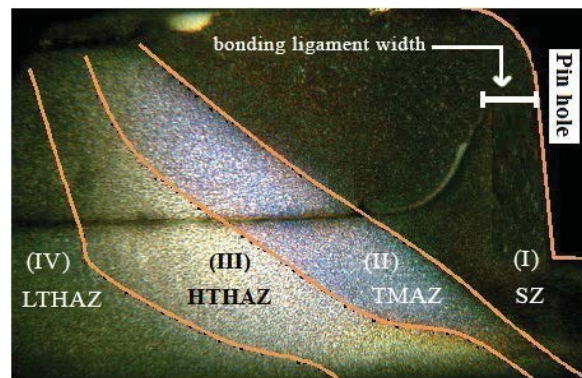


Fig. 6. The section view of joint at case B: (I) stir zone (SZ), (II) thermomechanically affected zone (TMAZ), (III) high temperature heat affected zone (HTHAZ) and (IV) low temperature heat affected zone (LTHAZ).

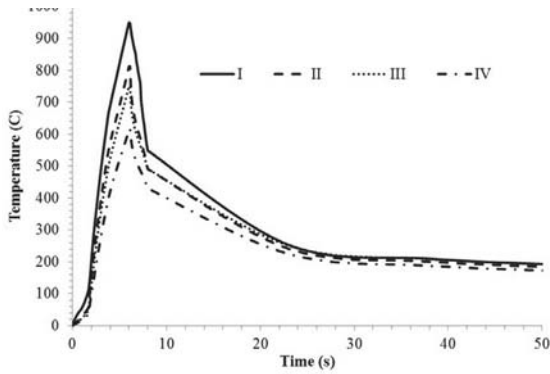
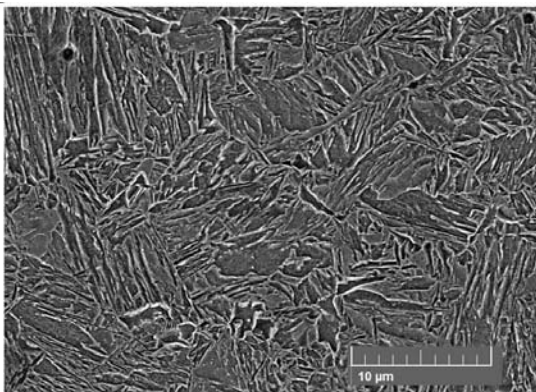


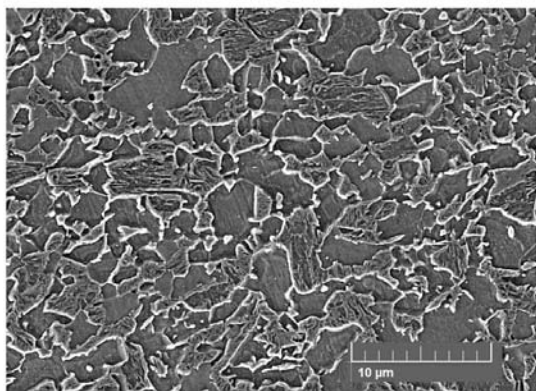
Fig. 7. Thermal histories of points from subdivided zones in case B.

Therefore, this zone can be called stir zone (SZ).

During cooling, the formation of bainite begins at the austenite grain boundary. It develops into a coarse feature through the coalescence of independently nucleated platelets which are in the same crystallographic orientation. It is possible that the formation of martensite-austenite constituent (MA) has been facilitated by the large amount of allotriomorphic ferrite. As the carbon solubility in ferrite is quite low,



(a)



(b)

Fig. 8. FE-SEM micrograph of (a) SZ and (b) TMAZ, at joint of case B.

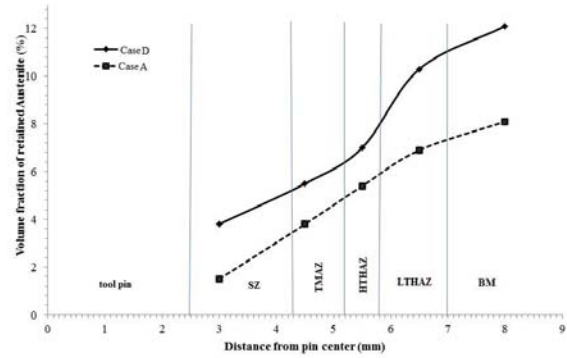


Fig. 9. Austenite volume fraction of subdivided welding zones in cases A and D.

there is an enrichment of the adjacent austenite with this element and with subsequent cooling, at M_s temperature, the formation of MA occurs.

The results of XRD analysis, which are shown in Fig. 9, show a very low volume fraction of austenite at this zone for cases A and D. It should be noted that the detection of the retained austenite by XRD, when it is less than 5%, is difficult and with error. Therefore, the amounts of 1.5% and 3.7% which are measured via XRD in cases A and D at SZ cannot be certain results. Thus, the microstructure of SZ for both cases was investigated using OM. Fig. 10 shows the OM micrograph of SZ in cases A and D. A small amount of the retained austenite in the SZ of case D can be observed, but it is not found in case A. It is reported that, this retained austenite is remnants of the base metal (BM) and not the austenite formed during heating^{2, 14}.

Fig. 11 represents the microhardness of welding zones in both cases. As can be seen in Fig. 11, the maximum hardness appears at SZ comparing to the other zones that resulted from the large amount of martensite. Also the microhardness of SZ in case A is a little more than case D which refers to higher amount of martensite and lower austenite.

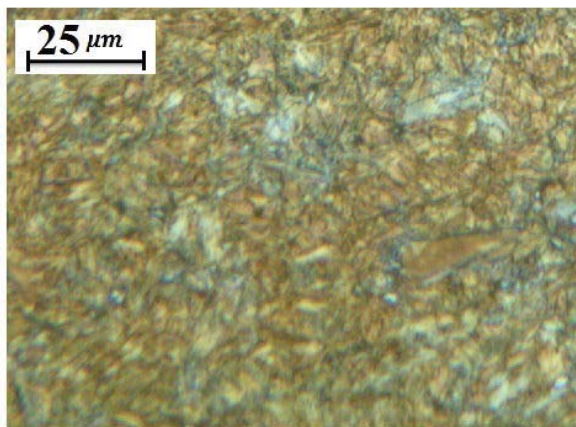
The microstructure of zone (II) which is shown in Fig. 8b includes ferrite, austenite, bainite and martensite and therefore, indicates that the material was heated to the peak temperature between A_{c3} and A_{c1} , where the ferrite and austenite coexist. During cooling, some of the austenite grains transformed into bainite and martensite. Moreover, the microstructure in zone (II) seems to be partly deformed as a result of light deformation imposed by the process in this zone, therefore this can be helpful for the mechanical stabilization of the austenite. This is reported that the grains with higher dislocation densities have higher stacking fault energy, resulting in lower driving force for martensitic transformation²⁷.

Thus, there are still austenite grains present in the microstructure in this zone. This retained austenite is remnants of the BM and not the austenite formed during heating².

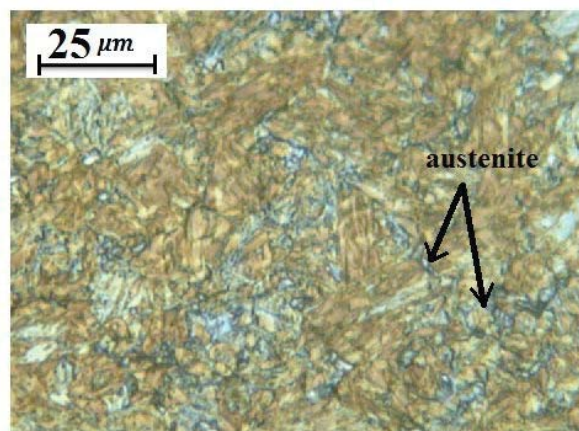
According to XRD results the volume fraction of this zone in welded cases increases comparing to SZ. According to the reasons were said for SZ, the volume fraction of the retained austenite in case D is more than case B. Because of simultaneous deformation and heat effects at zone (II), this region can be called thermomechanically affected zone (TMAZ).

Fig.12a shows the microstructure of zone (III) where ferrite and austenite can be observed mainly. In this zone, TRIP steel is heated up to the temperatures between Ac_1 and Ac_3 but without deformation and the austenite and ferrite is in equilibrium. This zone is a high temperature heat affected zone (HTHAZ). The microhardness decreases comparing to TMAZ because of the remarkable decreasing in martensite.

Fig.12b shows the microstructure of zone (IV) which the temperature is lower than Ac_1 and nominated as low temperature heat affected zone (LTHAZ). During the FSSW, when TRIP steel is subjected to the temperatures lower than Ac_1 , its influence on the microstructure is similar to the BIT step during the processing of TRIP steels. In BIT, bainite forms accompanied by carbon enrichment in the adjacent austenite phase^{2, 28}). According to Fig. 11



(a)



(b)

Fig. 10. OM micro-structure of SZ, (a) case A and (b) case D.

hardness of this zone is less than BM.

A temperature below Ac_1 may also induce tempering of the martensite, which is present in the BM before welding; this will lead to decreased hardness as well²⁹).

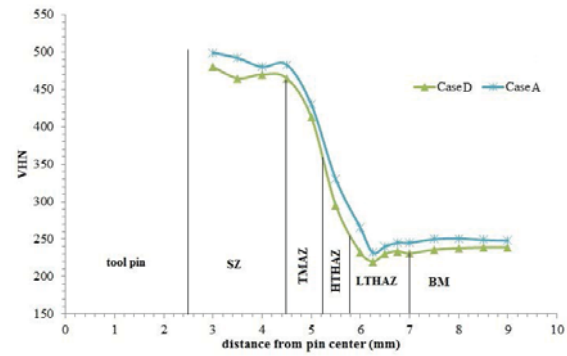
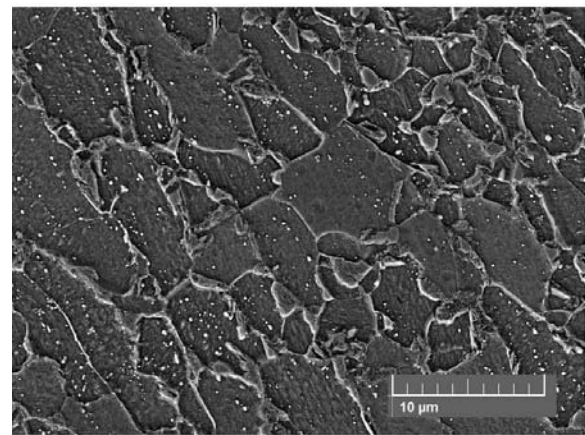
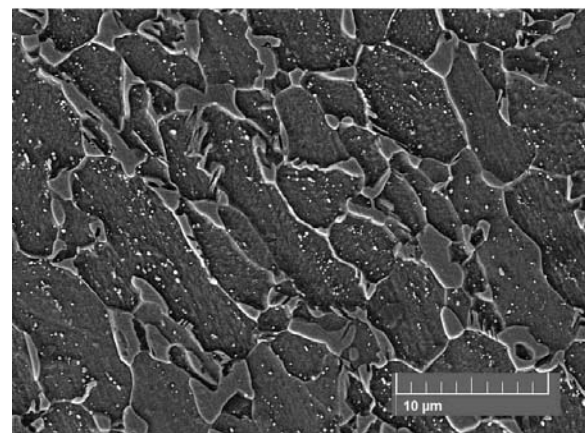


Fig. 11. Microhardness of subdivided zones and base metal in cases A and D.



(a)



(b)

Fig. 12. FE-SEM micrograph of: (a) HTHAZ and (b) LTHAZ, which include ferrite, bainite, martensite and the retained austenite.

In FSSW the strength of the weld emanates of the region where the two sheets are joined, which is commonly known as the bonding ligament width^{2,7}. The size and microstructure of bonding region have very important influences on the strength of the joint. Fig. 6 shows the bonding width at the FSSW of case D. The bonding region is a part of SZ. Tensile strength of the joint increases with the increasing of SZ size which can be controlled by FSSW parameters such as tool rotational speed, plunge depth, and dwell time. On the other hand, there are reports which indicate that not only the bonding ligament width is responsible for the strength, but also the type of the microstructure developed in the bonding ligament.

In this investigation, the welding parameters are constant in two cases and therefore only the initial microstructure of TRIP steels can play a role on the final microstructure and mechanical properties of the joints.

The strength of the welds was examined by lap shear tensile tests; the results for the cases A and D are shown in Fig. 13. It is clear that the strength of case D is higher than case A. Although the difference between the strength of the samples is very small but it is clear that there is a significant relationship between weld strength and the volume fraction of austenite. Since the weld strength is dependent on the bond area and the retained austenite in these areas are remnants of the BM^{2,14}) therefore, it can be concluded that the strength increases by increasing the amount of the primary retained austenite in the microstructure. In fact, with the increase of the initial retained austenite the amount of the retained austenite in the weld zones increases. Increasing the retained austenite in the weld zones causes occurring the TRIP effect (transformation of the retained austenite to martensite by strain) during tensile test and TRIP effect contributes to increasing the tensile strength.

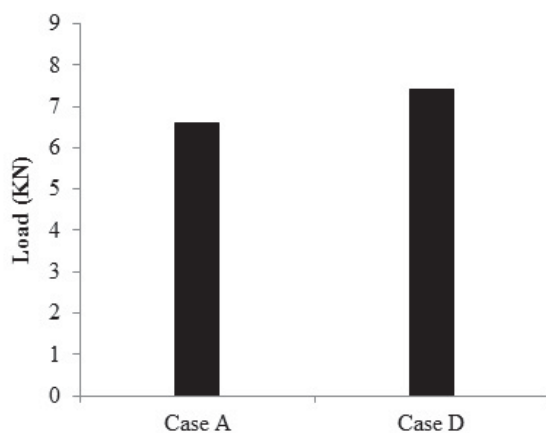


Fig. 13. Lap shear tensile strength of the welded cases A and D.

4. Conclusions

TRIP steels with the chemical composition of 0.21 C, 1.68 Mn, 1.5 Si, 0.03 Cr, 0.01 Ni, 0.016 Al and 0.009 S (wt.%) were fabricated by two-stage heat treatments including intercritical annealing at the temperatures of 770, 790 and 810 °C and isothermal bainitic transformation at the temperatures of 330, 350 and 370 °C. The cases with the maximum (12.1%) and minimum (8.1%) volume fractions of the retained austenite were chosen to investigate the effect of initial microstructure on weldability of TRIP steels.

Thus, these cases were joined by friction stir spot welding process under the same welding parameters. The effect of heat treatment conditions on the microstructure and mechanical properties of TRIP steels before and after welding were investigated:

- It was obtained that under the conditions of 790 °C /330 °C and 770 °C /350 °C the maximum and minimum amounts of the retained austenite resulted in the microstructure.
- The case that heat treated under the condition of 790 °C /330 °C had the best formability by showing the highest elongation (more than 40%) and the case that heat treated under the condition of 810 °C /350 °C had the highest tensile strength (more than 800 MPa).
- The volume fraction of the retained austenite of welded zones increased with increasing of the initial amount of austenite.
- As the microstructure of bonding region has an important influence on strength of FSSWed joints, the tensile strength of the joints increased with increasing of the initial retained austenite. With increasing the initial retained austenite the amount of retained austenite in the weld zones increased. Increasing the retained austenite in the weld zones caused occurring the TRIP effect (transformation of the retained austenite to martensite by strain) during tensile test. TRIP effect led to increasing the tensile strength.

References

- [1] M. Militzer: *Sci.*, 298(2002), 975.
- [2] T.C. Lomholt, Y. Adachi, J. Peterson, R. Steel, K. Pantleon, M.A. Somers: *Adv. Mat. Res.*, 409(2011), 275.
- [3] C. Mazzaferro, T. Rosendo, M. Tier, J. Mazzaferro, J. Dos Santos, T. Strohaecker: *Mater. Manuf. Process.*, 30(2015), 1090.
- [4] W.M. Thomas, E.D. Nicholas, J.C. Needham, M.G. Murch, P. Temple-Smith, C.J. Dawes: *International Patent Application PCT/GB92/02203 and GB Patent Application 9125978.8*, UK Patent Office, London, December 6, 1991.
- [5] A. Reilly, H. Shercliff, Y. Chen, P. Prangnell: *J. Mater. Process. Technol.*, 225(2015), 473.
- [6] M.J. Hsieh, Y.C. Chiou, R.T. Lee: *J. Mater. Pro-*

- cess. Technol., 224(2015), 149.
- [7] A.K. Lakshminarayanan, V.E. Annamalai, K. Elangovan: J. Mater. Res. Technol., 4(2015), 262.
- [8] Y. Chung, H. Fujii, R. Ueji, N. Tsuji: Scripta Mater., 63(2010), 223.
- [9] H. Fujii, R. Ueji, Y. Morisada, H. Tanigawa: Scripta Mater., 70(2014), 39.
- [10] T. Miura, R. Ueji, H. Fujii: J. Mater. Process. Technol., 216(2015), 216.
- [11] Y.F.Shena, L.N.Qiu, X.Sun, L.Zuo, P.K.Liaw, D.Raabe: Mater. Sci. Eng., A, 636(2015), 551.
- [12] J.J. Wang, S.v.d. Zwaag: Metall. Mater. Trans. A., 32 (2001), 1527.
- [13] J.H. Ryu, D.I. Kim, H.S. Kim, H.K.D.H. Bhadeshia, D.W. Suh: Scripta. Mater., 63(2010), 297.
- [14] M. Ghosh, K. Kumar, R.S. Mishra: Scripta. Mater., 63(2010), 851.
- [15] H. Fujii, R. Ueji, Y. Takada, H. Kitahara, N. Tsuji, K. Nakata, K. Nogi: Mater. Trans., 47(2006), 239.
- [16] H. Luo, H. Dong, M. Huang: Mater. Des., 83(2015), 42.
- [17] S. Lee, B.C.D. Cooman: Metall. Mater. Trans. A., 44(2013), 5018.
- [18] H.J. Jun, O. Yakubovsky, N. Fonstein: 1st Int. Conf. on High Manganese Steels, Seoul, Korea, (2011), A-5-1–A-5-13.
- [19] E.D. Moor, D.K. Matlock, J.G. Speer, M.J. Merwin: Scripta. Mater., 64(2011), 185.
- [20] E. Emadoddin, A. Akbarzadeh, G. Daneshi: Mater. Charact., 57(2006), 408.
- [21] J.O. Andersson, T. Helander, L. Höglund, P.F. Shi, B. Sundman, Thermo-Calc, Calphad, (2002) Computational tools for materials science.
- [22] R. Zhu, S. Li, I. Karaman: Acta. Mater., 60(2012), 3022.
- [23] H.K.D.H. Bhadeshia, program MAP_STEEL_MUCG83, (1983).
- [24] I. 14273, Specimen dimensions and procedure for shear testing resistance spot, seam and embossed projection welds, ISO Standard, (2002).
- [25] H.K.D.H. Bhadeshia, Bainite in Steels: Transformations, Microstructure and Properties, second ed., IOM Communications, (2001).
- [26] H.K.D.H. Bhadeshia, D. Edmonds: Acta. Metall., 28(1980), 1265.
- [27] J. Wan, S. Chen, T.Y. Hsu: J. Phys. IV., 381(2003), 112.
- [28] E. Girault, A. Mertens, P. Jacques, Y. Houbaert, B. Verlinden, J.V. Humbeeck: Scripta. Mater., 44(2001), 885.
- [29] A.K. Sinha, Physical Metallurgy Handbook, McGraw-Hill, (2002).